Supplementary Figures

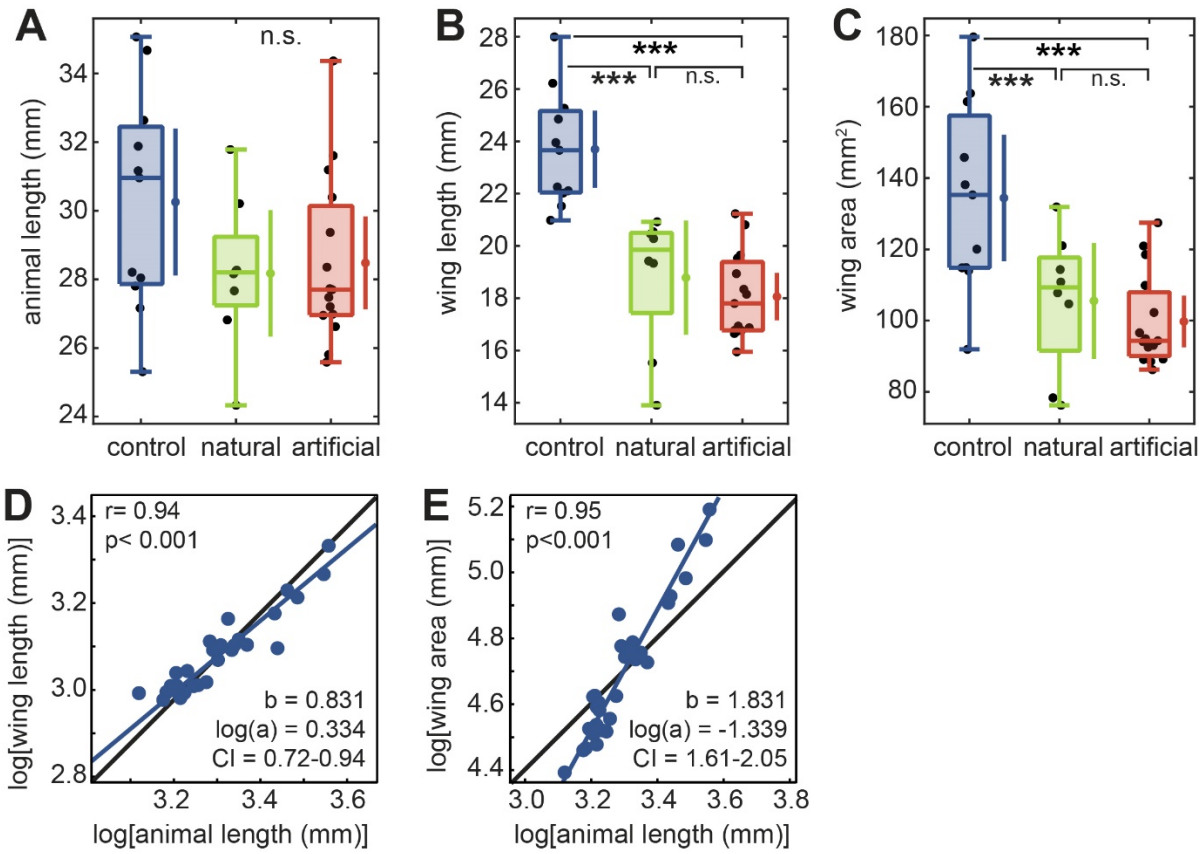

Figure S1. Body and wing anatomy of the different treatment groups. A Absolute length of the animals, measured from their anterior to posterior extent, **B** absolute length of the forewings from the wing base to the tip and **C** absolute wing area. Statistical differences between groups are indicated as: *** $p < 0.001$, ** $p < 0.01$, * $p < 0.05$, n.s. $p > 0.05$ (ANOVA with Tukey's HSD corrected post-hoc test was performed after confirming normality of residuals, see Table S1, *control*: n=11, *natural*: n=8, *artificial*: n=15). The dots next to each boxplot show the data's mean, and the lines around them the 95% confidence intervals around the mean. **D, E** Linear correlation between animal length and wing length (**D**) and wing area (**E**) on a logarithmic scale. r indicates the strength of the linear correlation, and p the statistical significance of the Pearson correlation coefficient, n=31. The allometric relationship was calculated using reduced major axis regression, where b is the exponential scaling exponent and log(a) is the log-transformed scaling constant of the allometric relationship. The 95% confidence interval of the slope is given by CI.

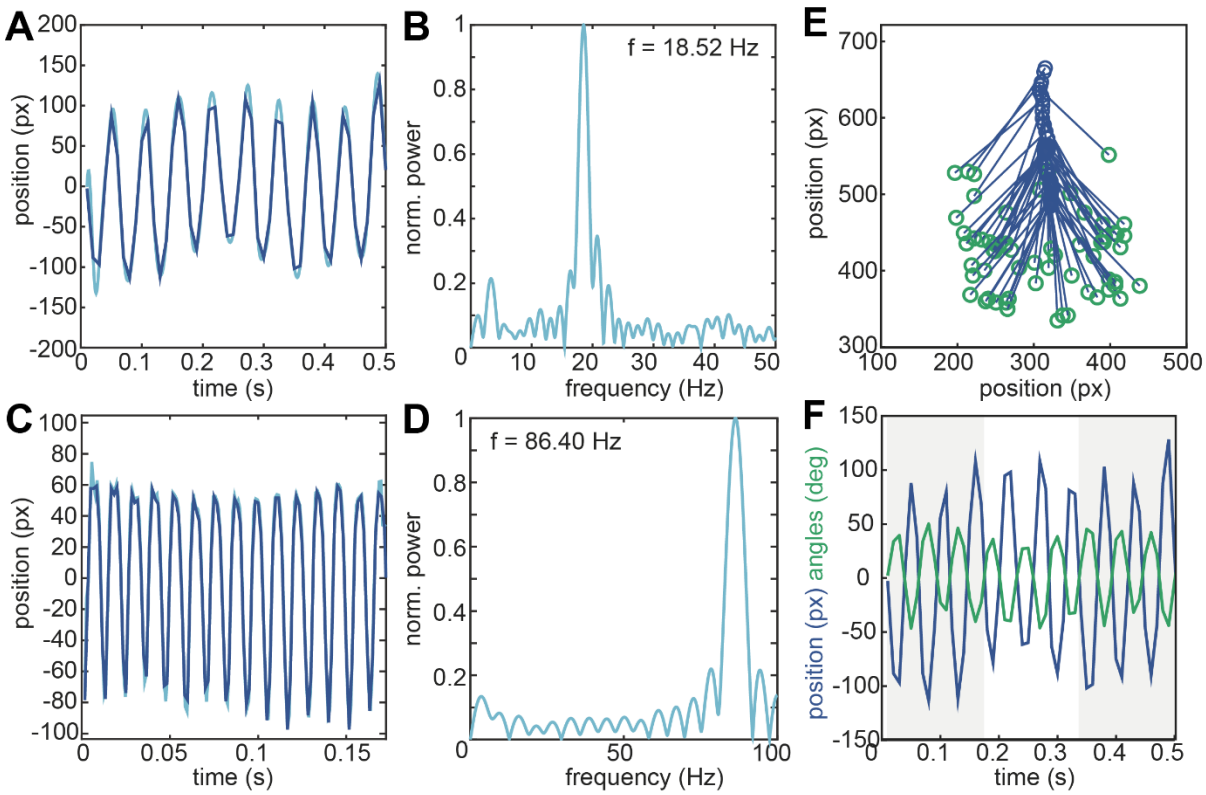

Figure S2. Wing beat frequency and amplitude measurements. A The wing beat of the animals in this study was measured by tracking the position of the tip of their wing for at least 100 frames. **B** The position data was then Fourier transformed and the wing beat frequency extracted as the peak in the power spectrum. Since the video frame rate of 100 fps resulted in a Nyquist frequency lower than the true wing beat frequency, the calculated frequency was subtracted from 100 Hz to obtain the real wing beat frequency. **C** The true wing beat frequency was measured in selected individuals using a frame rate of 600 fps. **D** Using this frame rate, the wing beat frequency was confirmed to range around 80 Hz, and thus exceed the Nyquist frequency at 100 fps. **E,F** Wing beat amplitude was calculated as the maximum angle between the most extreme wing positions measured over 5 consecutive wing beats, to avoid underestimating the real amplitude due to the temporal undersampling of the wing beat. **F** The wing tip position is shown in blue, the angles between the wing tip and body axis are shown in green.

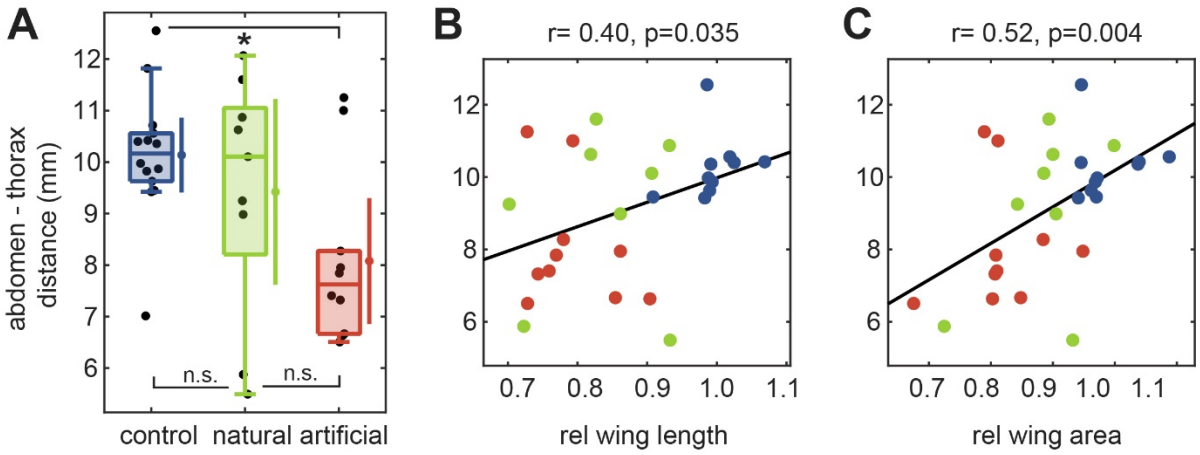

Figure S3. Body pitch angle of the different treatment groups. A We indirectly measured the pitch angle of the hawkmoth's body by comparing the distance between the thorax and the distal tip of the abdomen in the dorsal camera view while each hawkmoth was hovering at the artificial flower. Black dots denote average thorax – abdomen distance for each hawkmoth. Statistical differences between groups are indicated as: *** $p < 0.001$, ** $p < 0.01$, * $p < 0.05$, n.s. $p > 0.05$ (ANOVA with Tukey's HSD corrected post-hoc test was performed after confirming normality of residuals, Table S1, *control*: n=14, *natural*: n=9, *artificial*: n=10). **B,C** We furthermore tested for correlations between the thorax – abdomen distance and the relative wing length and the relative wing area. The strength of the linear correlation is given by r, and the statistical significance of the Pearson correlation coefficient by p (*control*: n=11, *natural*: n=8, *artificial*: n=10). The dots next to each boxplot show the data's mean, and the lines around them the 95% confidence intervals around the mean.

Supplementary Tables

Table S1 Statistical results of comparisons of population means / medians between the three damage conditions, using an ANOVA (df = 2) with Tukey's HSD corrected post-hoc test when normality of the residuals was confirmed (F-statistic), or a Kruskall-Wallis test (df = 2) with Tukey's HSD corrected post-hoc test (X^2-statistic) when it was not. Tested parameters are given in bold letters in the top row of each block of tests, the second row indicates the figures that show the corresponding data, and each last row per block indicates the number of individuals in each condition.

		animal length	**wing length**	**wing area**	**rel. wing length**	**rel. wing area**	**wing beat frequency**	**wing beat amplitude**	**angular velocity**	**thorax – abdomen distance**
		Fig.1 - S1A	Fig.1 - S1B	Fig.1 - S1C	Fig.1E	Fig.1F	Fig.2A	Fig.2B	Fig.2C	Fig.2 – S2A
test statistic, p-value		1.895 (F), 0.167	25.27 (F), <0.001	10.46 (F), <0.001	34.04 (F), <0.001	18.96 (F), <0.001	13.09(F), <0.001	25.35 (F), <0.001	35.59 (F), <0.001	4.10 (F), 0.0267
post-hoc p-values for:										
control	natural	0.228	<0.001	0.010	<0.001	0.070	0.070	0.013	0.004	0.607
control	artificial	0.228	<0.001	<0.001	<0.001	<0.001	<0.001	<0.001	<0.001	0.021
natural	artificial	0.963	0.707	0.781	0.381	0.083	0.083	0.007	<0.001	0.229
nr of individuals		11 8 15	11 8 15	11 8 15	11 8 15	11 8 15	17 10 15	17 10 15	17 10 15	14 9 10

		rel. lift force	**rel. mech. power**	**freq. – fix. ampl.**	**ampl. – fix. freq.**
		Fig.4A	Fig.4B	Fig.4E	Fig.4F
test statistic, p-value		0.103 (F), 0.903	0.016 (F), 0.984	27.05(F), <0.001	27.05 (F), <0.001
post-hoc p-values for:					
control	natural	0.953	0.998	0.004	0.004
control	artificial	0.897	0.983	<0.001	<0.001
natural	artificial	0.996	0.995	0.016	0.016
nr of individuals		11 8 15	11 8 15	11 8 15	11 8 15

		median displacement	**90% max. displacement**	**path length**	**total error**	**error 0.2 - 1.7 Hz**	**error 1.9 - 8.9 Hz**	**error = 1**
		Fig.5A	Fig.5B	Fig.5C		Fig.5D	Fig.5E	Fig.6F
test statistic, p-value		0.028 (X^2), 0.973	0.027 (F), 0.986	0.978 (F), 0.385	2.92 (X^2), 0.233	2.03 (F), 0.145	5.06 (X^2), 0.078	3.12 (F), 0.407
post-hoc p-values for:								
control	natural	0.986	0.989	0.617	0.238	0.135	0.225	0.691
control	artificial	0.973	0.989	0.386	0.489	0.403	0.087	0.385
natural	artificial	0.999	0.999	0.969	0.931	0.784	0.911	0.886
nr of individuals		17 10 15	17 10 15	17 10 15	17 10 15	17 10 15	17 10 15	17 10 15

Table S2 A Comparison of population medians of the estimated normalised lift force and normalised mechanical power generated with measured wing beat amplitude and the median wing beat frequency of the control group (*-f*), with the measured frequency and the median amplitude of the control group (*-a*) and with both median frequency and amplitude of the control (*-fa*) (shown in Fig. 5C,D) within each damage condition. The results of an ANOVA (df = 2) with Tukey's HSD corrected post-hoc test where normality of residuals could be confirmed, for all others conditions a Kruskall-Wallis test with Tukey's HSD corrected post-hoc test was performed. The last row gives the number of individuals in each condition. **B** Comparison of population medians of the estimated normalised lift force generated during hovering and the normalised mechanical power required for flapping versus 1 (shown in Fig. 5C,D) across damage conditions. The number of individuals in each condition are the same as in **A**. The results of a Wilcoxon signed rank test are shown, with the same sample sizes as given in **A**, and df = 7 the natural and df = 14 for the artificial condition.

A

			natural			artificial		
lift force	test statistic, p-value		6.9 (F), 0.005			36.3 (F), <0.001		
	post-hoc p-values for:							
	-f	**-a**	0.065			<0.001		
	-f	**-fa**	0.004			<0.001		
	-a	**-fa**	0.435			0.007		
power	test statistic, p-value		6.7 (F), 0.006			36.0 (F), <0.001		
	post-hoc p-values for:							
	-f	**-a**	0.066			<0.001		
	-f	**-fa**	0.005			<0.001		
	-a	**-fa**	0.454			0.013		
nr of individuals			**11**	**8**	**15**	**11**	**8**	**15**

B

signed rank, p-value		natural		artificial	
lift	**-f**	36	0.016	0	<0.001
	-a	37	0.008	0	<0.001
	-fa	40	0.008	0	<0.001
power	**-f**	37	0.016	0	<0.001
	-a	37	0.008	0	<0.001
	-fa	41	0.008	0	<0.001